Journal of Cerebral Blood Flow & Metabolism (2014) 34, 408–414

www.jcbfm.com

ORIGINAL ARTICLE

Regional cerebral blood flow and arterial blood volume and their reactivity to hypercapnia in hypertensive and normotensive rats

Tae Kim[1], J Richard Jennings[2] and Seong-Gi Kim[1,3,4]

Chronic hypertension induces cerebrovascular remodeling, changing the inner diameter and elasticity of arterial vessels. To examine cerebrovascular morphologic changes and vasodilatory impairment in early-stage hypertension, we measured baseline (normocapnic) cerebral arterial blood volume (CBV_a) and cerebral blood flow (*CBF*) as well as hypercapnia-induced dynamic vascular responses in animal models. All experiments were performed with young (3 to 4 month old) spontaneously hypertensive rats (SHR) and control Wistar–Kyoto rats (WKY) under ~1% isoflurane anesthesia at 9.4 Tesla. Baseline regional *CBF* values were similar in both animal groups, whereas SHR had significantly lower CBV_a values, especially in the hippocampus area. As *CBF* is maintained by adjusting arterial diameters within the autoregulatory blood pressure range, CBV_a is likely more sensitive than *CBF* for detecting hypertensive-mediated alterations. Unexpectedly, hypercapnia-induced *CBF* and blood-oxygenation-level-dependent (BOLD) response were significantly higher in SHR as compared with WKY, and the *CBF* reactivity was highly correlated with the BOLD reactivity in both groups. The higher reactivity in early-stage hypertensive animals indicates no significant vascular remodeling occurred. At later stages of hypertension, the reduced vascular reactivity is expected. Thus, *CBF* and CBV_a mapping may provide novel insights into regional cerebrovascular impairment in hypertension and its progression as hypertension advances.

Journal of Cerebral Blood Flow & Metabolism (2014) **34,** 408–414; doi:10.1038/jcbfm.2013.197; published online 20 November 2013

Keywords: arterial *CBV*; BOLD; *CBF*; cerebrovascular reactivity; hippocampus; hypertension

INTRODUCTION

The adaptive response of arterial vessels to chronic hypertension includes a narrowing of the lumen and an increase in wall thickness.[1,2] Consequently, cerebral arterial blood volume (CBV_a) and arterial vessel elasticity decrease, which may in turn alter arterial vascular reactivity to various stimuli. These cerebrovascular alterations could eventually lead to a regional reduction in cerebral blood flow (*CBF*) and tissue oxygenation,[3–5] thereby increasing the risk of stroke, vascular dementia, and cognitive decline.[6–8] However, early-stage alterations in the cerebrovasculature are easily modified. As the cerebral regulation of blood pressure differs from the systemic regulation, treatment aimed at reducing peripheral blood pressure may not provide the necessary therapy to prevent impairments of the brain vasculature. Therefore, the ability to detect the progression of hypertension and cerebrovascular remodeling by *in vivo* imaging is vital.

Hypertension-induced alterations in *CBF* have been assessed by magnetic resonance imaging (MRI), single-photon emission computed tomography and positron emission tomography, which reported a slight reduction in baseline (normocapnic) *CBF* in some,[8–10] but not in all hypertensive subjects.[1,11–14] In addition, studies showed that, as compared with normotensive subjects, hypertensive subjects have a blunted *CBF* response to neural tasks[11] and CO_2 stimulus.[15] In general, the brain maintains adequate *CBF* within a certain autoregulatory range independent of changes in systemic arterial pressure by adjusting vessel diameters of arteries and arterioles. In early-stage hypertension, *CBF* may maintain constant despite a decrease in CBV_a, before the compensation eventually fails. Thus, CBV_a may be a more sensitive index than *CBF* for identifying and assessing cerebrovascular risk factors in early-stage hypertension, and its reduction may be an early predictor of altered *CBF*.

In this study, we measured quantitative *CBF* and CBV_a, as well as cerebrovascular reactivity in a well-established hypertensive animal model (spontaneously hypertensive rats (SHR)) and a control model (Wistar–Kyoto rats (WKY)) to detect regional hypertensive cerebrovascular changes. Quantitative *CBF* was measured with arterial spin labeling (ASL) MRI, and quantitative CBV_a was obtained using magnetization transfer (MT)-varied MRI.[16–18] Varying the MT effect allowed us to separate MT-sensitive tissue from the MT-insensitive arterial blood signal.[16–18] Dynamic cerebrovascular reactivity as a response to hypercapnic manipulation was measured by blood-oxygenation-level-dependent (BOLD) functional magnetic resonance imaging in addition to *CBF* and CBV_a MRI. As BOLD functional magnetic resonance imaging is a vascular measure complementary to *CBF* and CBV_a, combining all three measures may provide important indices of vascular reserve and vessel viability.

MATERIALS AND METHODS

Animal Preparation and Hypercapnia Stimulation

All animal protocols were approved by the University of Pittsburgh Institutional Animal Care and Use Committee, in accordance with the National Institutes of Health Guide for the Care and Use of Laboratory Animals. A total of twenty four male rats were studied (Charles River Laboratories, Wilmington, MA, USA); twelve animals each for the SHR and

[1]Department of Radiology, University of Pittsburgh, Pittsburgh, Pennsylvania, USA; [2]Department of Psychiatry, University of Pittsburgh, Pittsburgh, Pennsylvania, USA; [3]Center for Neuroscience Imaging Research, Institute for Basic Science (IBS), Daejeon, Republic of Korea and [4]Department of Biological Sciences, Sungkyunkwan University, Suwon, Republic of Korea. Correspondence: Dr T Kim, Department of Radiology, University of Pittsburgh, 200 Lothrop Street, Pittsburgh, PA 15213, USA.
E-mail: tak19@pitt.edu
Source of funding: NIH: EB003375.
Received 10 July 2013; revised 15 October 2013; accepted 21 October 2013; published online 20 November 2013

WKY groups. All animals were used for baseline measurements, while ten SHR and eight WKY rats were used for hypercapnic challenge.

The animals were initially anesthetized with 5% isoflurane and intubated. Subsequently, the isoflurane level was reduced to 2% for surgery; the femoral artery and vein were catheterized to monitor arterial blood pressure and to administrate supplemental fluid, respectively. The isoflurane level was then reduced to ~1% with air supplemented with O_2 to attain a total O_2 level of ~30% throughout experiment, which assists maintaining a normal PaO_2 level under anesthesia. The head of the animal was carefully secured in a home-built restrainer before placement in the magnet. During experiments, mean arterial blood pressure (MABP), end-tidal CO_2 ($EtCO_2$), O_2, and isoflurane level were continuously monitored and recorded with Acqknowledge software (MP150, BIOPAC Systems, Goleta, CA, USA). Blood gases were measured (Stat profile pHOx, Nova Biomedical, Waltham, MA, USA) and ventilation rate and volume were adjusted accordingly. Body temperature was monitored by a rectal probe and maintained at 37 to 37.5°C with a feedback hot water circulator.

Thirty-second CO_2 stimulation was performed by switching ventilation gas mixtures of air with 30% oxygen without and with ~4% CO_2 using an electronically controlled pneumatic valve. An inter-hypercapnia interval was >15 minutes. It should be noted that as longer stimulation and higher CO_2 level require a longer inter-stimulus delay for returning to the baseline physiologic condition, the relatively short stimulus duration and mild hypercapnia were used for repeating experiments rapidly.

Magnetic Resonance Acquisitions

All studies were performed at a magnetic field strength of 9.4T with 310 mm diameter of bore size, interfaced to a Unity INOVA console (Varian, Palo Alto, CA, USA). The actively shielded gradient coil had an inner diameter of 120 mm with a gradient strength of 4 G/mm and a rise time of 130 microseconds (Magnex, Abingdon, UK). Two actively detunable radiofrequency (RF) coils were used: a butterfly-shaped surface coil positioned in the neck region for continuous ASL, and a surface coil of 23 mm diameter positioned on top of the head for tissue saturation via MT effects and for image acquisition. A three-dimensional anatomic image was acquired using a magnetization prepared rapid acquisition gradient echo sequence with TR = 10 milliseconds, TE = 5 milliseconds, TI = 1.4 seconds, and a voxel resolution of $117 \times 117 \times 117\ \mu m^3$. From the three-dimensional image, five 2-mm thick coronal slices were selected for cerebrovascular imaging. To compare with cerebrovascular images, T_2-weighted 2-D images were then acquired in the same slices with TR = 2 seconds, 8 echoes with 11-millisecond spacing, and an in-plane resolution of $58 \times 58\ \mu m^2$.

All physiologic images were acquired using the single-shot spin-echo echo planar imaging (EPI) technique with an in-plane resolution of $469 \times 469\ \mu m^2$, TE = 18 milliseconds, and TR = 3 seconds. A 2.75-second magnetization preparation period was used for applying ASL and MT-inducing RF pulses as described previously.[19] Each experimental set included four ASL runs to obtain *CBF* and CBV_a with improved temporal resolution; two runs each with two different MT saturation levels. In each ASL run, arterial spin labeled (lab) and control unlabeled (unlab) images were acquired repeatedly in an interleaved manner. The acquisition order of labeled (lab) and unlabeled (unlab) images was changed in alternate runs to increase the temporal resolution of the ASL data. The targeted MT saturation level was obtained by adjusting the power level of MT-inducing radiofrequency pulses with +8500 Hz off-resonance frequency; MT ratios (*MTR*) were $(1 - S_{sat}/S_0) = 0$ and 0.5, where S_{sat} and S_0 are the equilibrium signal in the presence and absence of MT saturation. Each CO_2 challenge run consisted of 150-second pre-stimulation (25 lab and unlab images), 30-second hypercapnic stimulation (5 pair images), and 450-second post stimulation (75 pair images). Four to six experimental sets (16 to 24 runs) were obtained in each animal. For animal studies without CO_2 challenge, a similar number of images were also acquired.

Data Processing

Data analysis was performed with STIMULATE (CMRR, http://www.cmrr.umn.edu/stimulate, Minneapolis, MN, USA), ImageJ (NIH, http://rsb.info.nih.gov/ij, Bethesda, MD, USA), and in-house Matlab routines (Mathworks, Natick, MA, USA). For each study, all runs with identical experimental conditions were averaged to generate group data. As two different orders of ASL and control image acquisition with 6-second temporal resolution were used, the practical temporal resolution was 3 seconds.[19]

Cerebral blood flow and CBV_a maps were obtained, and regional baseline values and evoked responses were determined in a region-by-region basis. To select regions of interest (ROIs), 2-D anatomic images were generated from the three-dimensional anatomic image to match five-slice cerebrovascular maps. Then, five ROIs corresponding to the sensory cortex, motor cortex, caudate putamen, thalamus, and hippocampus were carefully and conservatively delineated on each of the five-slice anatomic images in both hemispheres, based on a rat atlas.[20] Pixels with anatomic variations within the slice, such as those coinciding with the hippocampal and ventricle boundaries, were easily visualized with the high-resolution three-dimensional data, and not included. All pixels within each ROI were averaged for each subject's ROI analysis. Individual subject results were averaged and group data are reported as mean ± s.d. A two-sample equal variance *t*-test was performed for statistical significance for the difference between both animal groups.

Baseline cerebral blood flow and cerebral arterial blood volume. For baseline *CBF* and CBV_a measurements, all repeated ASL data were averaged during the pre-CO_2 challenge period, or an all period in case of no CO_2 challenge, resulting in one labeled and one unlabeled control image for *MTR* = 0 (no MT effect), and *MTR* = 0.5. Details of data processing were described previously.[16,17] Briefly, the ASL signals ($\Delta S_{ASL,MT}$) were obtained from the difference between control and labeled images for each *MTR* level. The CBV_a signal was separated from $\Delta S_{ASL,MT}$ using the different MT effects in tissue versus arterial blood. This is possible because tissue signals are selectively reduced by MT, while the arterial blood pool experiences only a minimal MT effect owing to the fast and continuous inflow of fresh blood spins from outside the region of the MT-inducing radiofrequency coil's coverage. Normalized $\Delta S_{ASL,MT}$ signals ($\Delta S_{ASL,MT}/S_0$) were linearly fitted against normalized control signals (S_{MT}/S_0), where S_0 is the signal intensity from the control image with *MTR* = 0. Cerebral blood flow (in units of mL/g per second) without any arterial blood volume contribution was determined from the slope of the linear fitting as

$$CBF = \frac{\lambda}{T_1} \cdot \left(\frac{slope/\zeta}{2\alpha_c - slope/\zeta}\right), \quad (1)$$

where λ is the tissue–blood partition coefficient of 0.9 mL/g;[21] T_1 is the T_1 value of tissue without MT and in the absence of *CBF* contributions; α_c is the labeling efficiency of arterial spins at the capillary exchange site within the imaging slice, calculated as $\alpha_0 \cdot \exp(-\tau_c/T_{1a})$, where α_0 is the labeling efficiency at carotid artery = 0.525 and τ_c is the blood transit time from carotid artery to exchange site = 0.6 seconds;[22] and ζ is the correction factor to the steady state, which is $(1\text{-}\exp(-T_{lab}/T_{1app}))$, where T_{lab} is the time span for the spin-preparation period = 2.75 seconds and T_{1app} (apparent T_1) = 1.9 seconds.[23]

Quantitative CBV_a (in units of mL/g) was obtained from the intercept and slope of the linear fitting as

$$CBV_a = \lambda \times intercept/(2a_a - slope), \quad (2)$$

where α_a is the labeling efficiency of spins entering the imaging slice, calculated as $\alpha_0 \times exp(-\tau_a/T_{1a})$, where τ_a is the blood transit time from carotid artery to imaging slice = 0.3 seconds[22] and T_{1a} is T_1 value of arterial blood = 2.3 seconds at 9.4 T.[17]

Dynamic changes in blood-oxygenation-level-dependent, cerebral blood flow, and cerebral arterial blood volume to hypercapnia. Hypercapnia-induced relative BOLD and *CBF* changes were obtained from control and ASL images, respectively, in the run without MT effect (*MTR* = 0). To obtain dynamic CBV_a changes induced by CO_2 stimulation, values should be determined for each time point. However, only 4 to 6 runs were averaged, so this data did not have sufficient sensitivity to reliably quantify CBV_a using the MT-varied ASL method. Instead, hypercapnia-induced CBV_a changes were calculated with the MT-varied BOLD method.[16,18,24] The CO_2 stimulus-induced signal change normalized by S_0 ($\Delta S_{BOLD,MT}/S_0$) was linearly fitted against the normalized baseline signal, S_{MT}/S_0. The absolute change of CBV_a (in units of mL/g) was obtained from the intercept, as $\Delta CBV_a = \lambda \times$ intercept.

Hypercapnia-induced hemodynamic responses did not reach the steady state (i.e. plateau) because of the 30-second stimulation; mean reactivity values for each animal were determined by averaging the hypercapnic period, which was defined from corresponding hemodynamic response as a time period between 6 seconds before the peak and 24 seconds after the peak, which is agreeing with ~90% and ~80% of the peak of BOLD response, respectively, for every measurements.

RESULTS

During the experiments, all animals were maintained within normal physiologic ranges. Throughout the study, physiologic conditions were similar between WKY and SHR; pH = 7.48 ± 0.05 and 7.50 ± 0.03, $PaCO_2$ = 34.9 ± 3.54 mm Hg and 31.3 ± 3.47 mm Hg, PaO_2 = 116 ± 13 mm Hg and 133 ± 24 mm Hg, $EtCO_2$ before hypercapnic challenge = 3.23 ± 0.31% and 3.53 ± 0.33%, SO_2 = 97.8 ± 1.6% and 98.7 ± 0.6%, Hct = 36.8 ± 2.39% and 37.8 ± 2.33%, body weight = 325 ± 39 g and 321 ± 45 g, and age = 16.7 ± 3.2 and 14.7 ± 2.6 weeks, respectively. However, the two groups had a significantly different MABP = 98 ± 11 mm Hg in WKY versus 148 ± 18 mm Hg in SHR ($P < 0.0001$). These MABP levels did not change during CO_2 stimulation.

We evaluated the *CBF* and CBV_a in the hypertensive and normotensive groups. Figure 1 shows T_2-weighted anatomic images and quantitative maps of *CBF* and CBV_a from one WKY and one SHR under the baseline condition (without CO_2 stimulation). In T_2-weighted images, ventricle areas indicating hyperintensity were enlarged in SHR, which is consistent with previous findings.[25–27] Interestingly, *CBF* maps were similar for both groups, but SHR had much smaller CBV_a values as compared with WKY. To determine similarities and differences between WKY and SHR, we conservatively chose five ROIs (see Figure 1A), and calculated their *CBF* and CBV_a values (Figure 2). As expected from the *CBF* maps (Figure 1B), *CBF* values between the two groups were not significantly different (Figure 2A), despite a small difference in

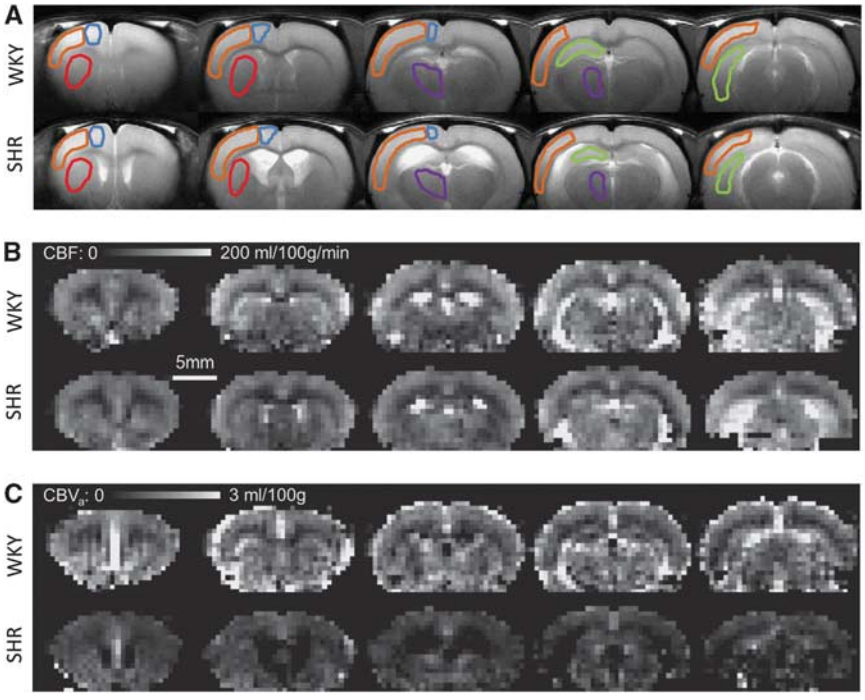

Figure 1. Anatomic T_2-weighted images (**A**) and quantified cerebral blood flow (*CBF*) (**B**) and cerebral arterial blood volume (CBV_a) (**C**) maps from Wistar–Kyoto rats (WKY) and spontaneously hypertensive rats (SHR). Data from one representative animal for each group are shown. The volume of hyperintense ventricles increased in SHR. Overall, both animal models had similar *CBF* values, whereas SHR demonstrated smaller CBV_a values than WKY. Five regions of interest were chosen in both hemispheres, but overlaid on one hemisphere in the anatomic images; sensory cortex—orange; motor cortex—blue; caudate putaman—red; thalamus—purple; hippocampus—green.

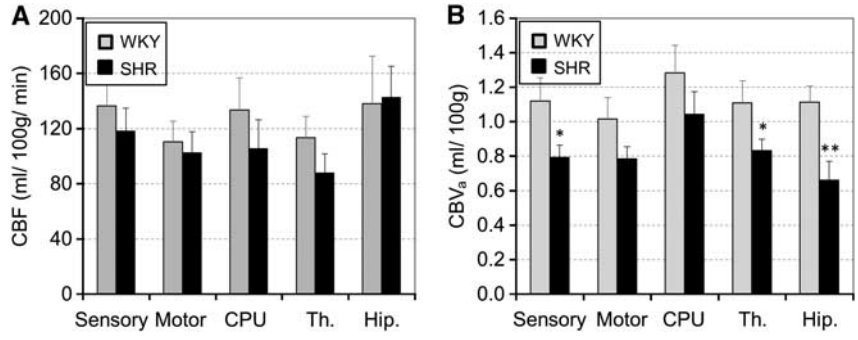

Figure 2. Baseline cerebral blood flow (*CBF*) (**A**) and cerebral arterial blood volume (CBV_a) (**B**) of five regions of interest (ROIs) under the normocapnic condition. All 12 animal data for each group were averaged. Spontaneously hypertensive rats (SHR) had slightly lower *CBF* values as compared with Wistar–Kyoto rats (WKY), whereas CBV_a values were signtificantly lower in most areas, particularly in the hippocampus (*$P < 0.05$, **$P < 0.01$). Error bars: s.e.m. ($n = 12$); CPU, caudate putamen; Th, thalamus; Hip, hippocampus.

baseline $PaCO_2$. However, CBV_a values from SHR were lower than those from WKY in all five regions. The largest reduction of CBV_a responding to hypertension was observed in the hippocampus, indicating that region-dependent cerebrovascular changes indeed occur.

Dynamic $EtCO_2$ responses induced by 30-second hypercapnia are plotted in Figure 3. The baseline $EtCO_2$ level was slightly lower for WKY than for SHR. Owing to a long air delivery system, $EtCO_2$ changed around 30 seconds after switching to a gas mixture with 4% CO_2, but dynamic $EtCO_2$ response was reproducible and consistent across all animals studied. The peak $EtCO_2$ change was ~1.8% to 2.1%, equivalent to ~14 to 16 mm Hg in our anesthetized condition, which is higher than self-breathing awake human studies. The evoked $EtCO_2$ change was slightly higher for WKY than for SHR.

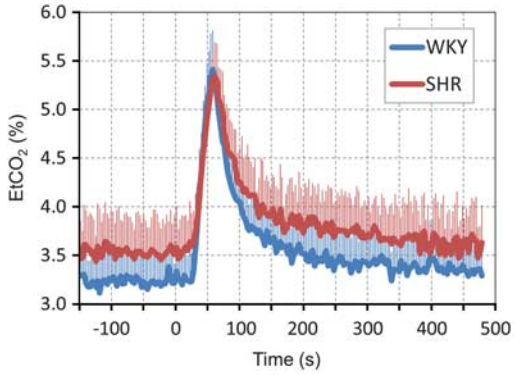

Figure 3. End-tidal CO_2 ($EtCO_2$) responses to CO_2 stimulation. All animal data were averaged. Inhalation of ~4% CO_2 in a gas mixture of air with 30% oxygen began at time 0 and continued for 30 seconds; however, there was a delay owing to a long gas delivery system to the animal inside the magnet. In all animals, dynamic end-tidal CO_2 responses were quite similar. Error bars: s.e.m. SHR, spontaneously hypertensive rats; WKY, Wistar–Kyoto rats.

Hypercapnic challenge activated most pixels (75% to 95% of pixels for $P<0.05$) in all ROIs (data not shown). However, to minimize pixel selection bias for the comparison between SHR and WKY, all pixel values within each ROI were averaged for each animal. Group-averaged time courses of BOLD, rCBF, and ΔCBV_a responses to hypercapnia are plotted in Figure 4. All regions had similar temporal patterns, so data of the sensory cortex and hippocampus ROIs are shown as representatives. Generally, the dynamics of BOLD and *CBF* responses were similar between SHR and WKY. Although a temporal resolution of 3 seconds did not allow us accurate analyses of dynamic properties, the time-to-peak of ΔCBV_a appeared shorter for the SHR animals.

The amplitude changes of BOLD, rCBF, and ΔCBV_a were obtained from hypercapnic data, and ΔCBF and relative CBV_a were calculated with baseline *CBF* and CBV_a. Group-averaged hypercapnia-induced BOLD, rCBF, relative CBV_a, ΔCBF, and ΔCBV_a are shown in Figure 5. Unlike higher evoked $EtCO_2$ change for WKY versus SHR (see Figure 3) and similar baseline *CBF* values, SHR demonstrated a much larger BOLD and rCBF reactivity to hypercapnia than WKY in all five regions ($P<0.01$). However, ΔCBV_a to hypercapnia did not show any difference between the two models (Figure 5E), but relative CBV_a change was slightly higher for SHR than for WKY even though it was not statistically significant.

Blood-oxygenation-level-dependent and rCBF reactivity was highly correlated in both groups (Figure 6). The ratio of BOLD (%) to rCBF (%) (= BOLD/rCBF) were similar for WKY versus SHR; 0.039 ± 0.008 versus 0.036 ± 0.004 for sensory, 0.030 ± 0.009 versus 0.032 ± 0.009 for motor, and 0.029 ± 0.003 versus 0.027 ± 0.005 for the hippocampus, and slightly different for CPU, 0.023 ± 0.002 versus 0.030 ± 0.005 and for the thalamus, 0.025 ± 0.003 versus

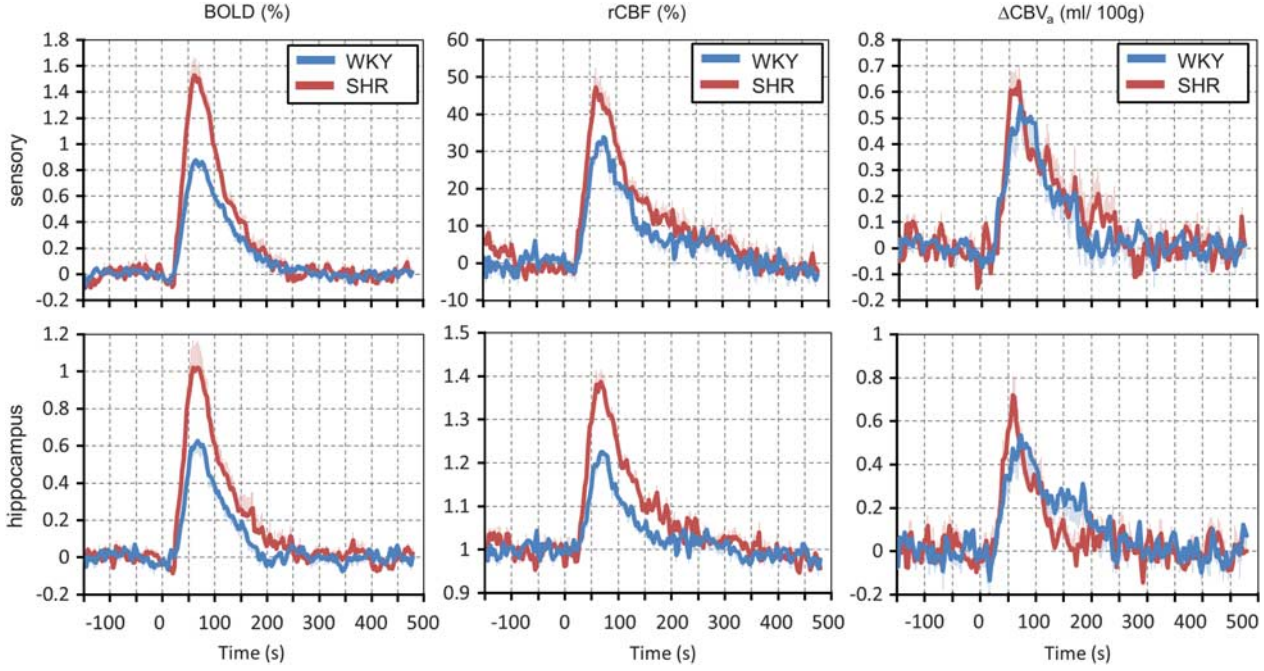

Figure 4. Group-averaged blood-oxygenation-level-dependent (BOLD) (left), relative cerebral blood flow (rCBF) (middle) and cerebral arterial blood volume (ΔCBV_a) (right) responses of the sensory (upper) and the hippocampus area (lower) to CO_2 stimulation. The dynamics of BOLD and ΔCBF were similar, but their peak response was much higher for spontaneously hypertensive rats (SHR). The ΔCBV_a responses in SHR appeared to have a slightly shorter time-to-peak and faster return with similar amplitude of signal changes. Error bars: s.e.m.. WKY, Wistar–Kyoto rats.

0.035 ± 0.012. This indicates that the BOLD reactivity is a good index of *CBF* reactivity.

DISCUSSION

We investigated the regional cerebrovascular similarities and differences between SHR and normotensive controls using MRI techniques. These studies revealed several major findings: (1) both animal models had similar *CBF* values, but SHR had a smaller regional CBV_a value than WKY; and (2) in response to CO_2, SHR displayed greater *CBF* and BOLD reactivity than WKY, but both groups had a similar ΔCBV_a.

Before we discuss the biologic implications of our studies, it is important to evaluate our methodologies critically. There are several concerns. (1) One concern is whether baseline *CBF* versus CBV_a can be compared fairly owing to potentially different sensitivities. Both *CBF* and CBV_a were obtained from exactly the same data sets using equations (1) and (2), respectively. Cerebral blood flow was calculated from the slope, whereas CBV_a was determined primarily from the intercept of linear fitting, as the slope is much less than $2\alpha_a$ in equation (2). As only two points were used for fitting, fitting errors could not be determined. The ratio of pixel-wise SNR between (slope/T_1) and intercept was 1.62, thus the error of CBV_a would be higher than that of *CBF*. As *CBF* values were similar for SHR and WKY, higher errors in CBV_a would induce less significant changes between the two animal models. However, the inter-animal variations of *CBF* and CBV_a were similar (Figure 2), possibly due to a small error in ROI values. Consequently, significant baseline CBV_a differences between two models cannot be explained by measurement error. (2) In our hypercapnic studies, different data sets were used; rCBF from ASL data (i.e., unlabeled—labeled) without MT, BOLD from unlabeled data without MT, and ΔCBV_a from unlabeled data with and without MT. While both rCBF and BOLD responses were obtained directly by comparing values at baseline versus stimulation, ΔCBV_a was from comparing intercepts of linear fitting. Further, less signal averaging was performed for dynamic studies compared with baseline measurements. Consequently, ΔCBV_a is more prone to errors than BOLD and *CBF* responses. (3) As we used a relative short hypercapnic challenge, hemodynamic responses did not reach to a steady state. Thus, the averaged amplitudes measured during dynamic–hemodynamic changes were less than steady-state values, which were used in a major portion of the literature. However, relative reactivity values between two different animal models and between different vascular parameters were still valid.

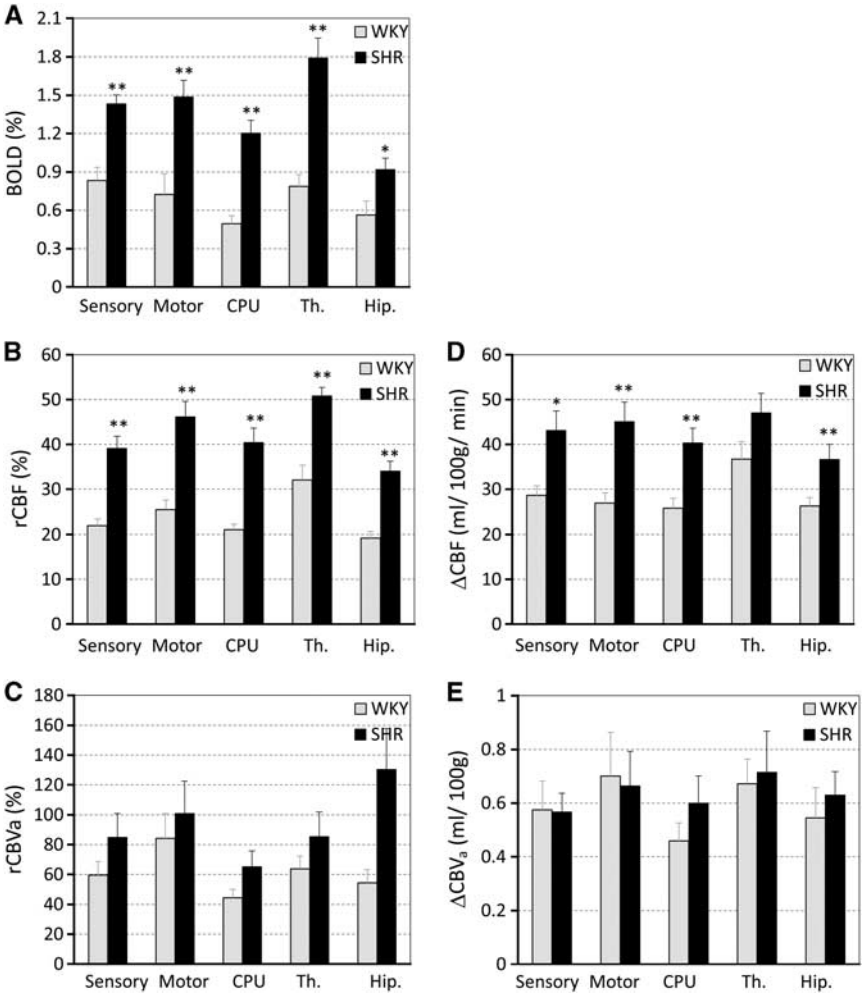

Figure 5. Blood-oxygenation-level-dependent (BOLD) (**A**), relative cerebral blood flow (rCBF) change (**B**), relative cerebral arterial blood volume ($rCBV_a$) change (**C**), ΔCBF (**D**) and ΔCBV_a (**E**) during CO_2 stimulation. Hypercapnia-induced BOLD and rCBF responses in spontaneously hypertensive rats (SHR) were significantly higher than those in Wistar–Kyoto (WKY) rats in all regions examined (*$P < 0.05$). ΔCBV_a responses between both groups were similar, whereas relative CBV_a responses appeared higher for hypertensive animals. Error bars: s.e.m.; CPU, caudate putamen; Th, thalamus; Hip, hippocampus.

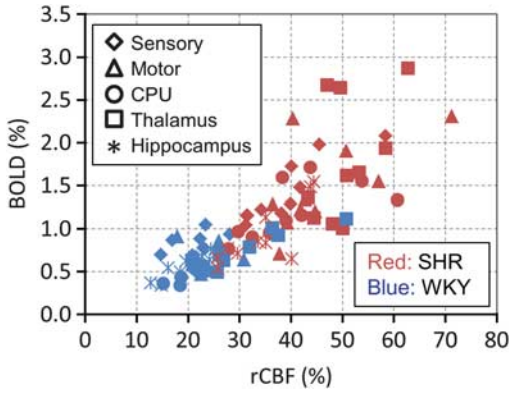

Figure 6. Relationship between the hypercapnia-induced blood-oxygenation-level-dependent (BOLD) response and relative cerebral blood flow (rCBF) changes. This graph includes data from all five regions of interest (ROIs) (different symbols) in all of the animals. Blood-oxygenation-level-dependent responses were linearly correlated with rCBF changes in both spontaneously hypertensive rats (SHR) (red symbols) and Wistar–Kyoto rats (WKY) (blue symbols). This indicates that BOLD is a good index of *CBF* reactivity, as no oxygen consumption is expected.

Our results show that hypertensive animals have a reduction in CBV_a as expected given the previous study that employed a microscope methodology.[28] Increased MABP (hypertension) induces the constriction of arterial vessels to maintain the same *CBF* level. Therefore, CBV_a can act as a key indicator for the detection of regional cerebrovascular changes in hypertension. Interestingly, we found that hypertension significantly altered the CBV_a of the hippocampus, an area involved in learning and memory. This cerebrovascular alteration may be related to the hypoxia and neural loss in the hippocampus of SHR, leading to vascular dementia.[29]

We also observed a similar baseline *CBF* in SHR and WKY animals, consistent with some human studies[1,11–14] but not others in which hypertensive subjects demonstrated a slight reduction in *CBF*.[8–10] At the same time, in other studies using the SHR and WKY models, hypertensive animals had a much higher baseline *CBF* value than control animals under 2% isoflurane (104 ± 23 versus 71 ± 19 mL/100 g per minute[30] and 150 ± 20 versus120 ± 20 mL/100 g per minute.[31]) However, the fact that we used $\sim$1% isoflurane while the other studies used 2% may account for this difference in results.[30] The 2% isoflurane level, typical for surgical procedures, could impair cerebrovascular regulation during a long experiment. Indeed, Leoni *et al*[30] and colleagues observed a decrease in MABP during hypercapnia in animals anesthetized with 2% isoflurane, unlike our study. As *CBF* is maintained within a certain autoregulatory range independent of changes in systemic arterial pressure through the adjustment of artery and arteriole diameters,[3,32] *CBF* may not be a sensitive marker of early hypertension.

As the evoked $EtCO_2$ change was slightly higher for WKY than for SHR, the reactivity of WKY would be higher than that of SHR, if the magnitude of $EtCO_2$ change is directly related to vascular reactivity. Contrary to the expectation from $EtCO_2$ change, we found that hypercapnia induced greater *CBF* and BOLD responses in hypertensive animals, while both hypertensive and control rats showed a similar increase in ΔCBV_a (Figure 5). The *CBF* change is expected to be associated with the CBV_a change. Even though hypercapnia-induced ΔCBV_a is similar for the both animal models, baseline CBV_a is lower for SHR than WKY. Consequently, the relative CBV_a change is higher for SHR than WKY, leading to much higher *CBF* and BOLD responses for hypertensive rats. Higher vascular reactivity under the vasoconstricted hypertensive condition is similar to the increased reactivity under the vasoconstricted hypocapnic condition in normal subjects,[33] indicating that the SHR model used in our studies did not impair vascular viability.

Our observations differ from human ^{15}O water positron emission tomography studies in which hypertensive subjects demonstrated a blunted *CBF* response to neural tasks as compared with normotensive age-matched 60-year-old subjects.[11] This reduction in *CBF* response may be the result of a decrease in neural activity and/or neurovascular reactivity, possibly confounded by age-related vasodilatory deterioration. Based on blood flow velocity measurements with transcranial Doppler sonography, Meada *et al*.[15] noted that hypertensive subjects have decreased CO_2 reactivity in the middle cerebral artery. In contrast, the reactivity measured with a ^{133}Xe carotid angiogram is similar between hypertensive and normotensive subjects, either during CO_2 inhalation or during hyperventilation.[34] These large vessel measurements would be expected to differ from our measurements in small cortical arteries and arterioles given that these small vessels undergo hypertrophy in chronic hypertension.[35] The disparity between human and animal studies may cause differences. Anesthesia is needed to minimize head motion and stress levels during animal experiments, but anesthetics affect the vasculature and possibly the blood pressure. However, the mild isoflurane anesthesia ($\sim$1%) used in this study produced no significant blood pressure changes in either SHR or WKY strains over the duration of the experiment. One possible scenario for discrepancy is that arterial vessels have not yet undergone significant remodeling in our hypertensive animals; thus, vascular reactivity is not compromised. Taking our current and previously reported data together, we hypothesize that the hyperreactivity at an early hypertensive stage without significant arterial remodeling is followed by the hyporeactivity at a later hypertensive stage due to arterial vessel wall thickening and remodeling. Vascular reactivity may be used to determine whether vascular remodeling is significant. Further longitudinal studies are necessary for examining our hypothesis.

As histopathological findings and morphologic damage induced by cerebrovascular alterations in the hypertensive animal brain have been shown to be very similar to those observed in the human brain,[29,36–39] similar cerebrovascular morphologic and functional changes are expected in hypertensive patients. The noninvasive MRI mapping technique would be helpful to understand cerebrovascular physiology of hypertension progression and to guide intervention optimized to combat both systemic and cerebrovascular hypertensive impairments.

DISCLOSURE/CONFLICT OF INTEREST

The authors declare no conflict of interest.

REFERENCES

1 Baumbach GL, Heistad DD. Cerebral circulation in chronic arterial hypertension. *Hypertension* 1988; **12**: 89–95.
2 Laurent S, Boutouyrie P, Lacolley P. Structural and genetic bases of arterial stiffness. *Hypertension* 2005; **45**: 1050–1055.
3 Iadecola C, Davisson RL. Hypertension and cerebrovascular dysfunction. *Cell Metab* 2008; **7**: 476–484.
4 Jennings JR, Zanstra Y. Is the brain the essential in hypertension? *Neuroimage* 2009; **47**: 914–921.
5 Novak V, Hajjar I. The relationship between blood pressure and cognitive function. *Nat Rev Cardiol* 2010; **7**: 686–698.
6 Gautier JC. Cerebral Ischemia in Hypertension. *In: Vascular Disease of the Central Nervous System*. Churchill Livingstone: Edinburgh, London, 1983.
7 Hazama F, Amano S, Haebara H, Yampri Y, Okamoto K. Pathology and pathogenesis of cerebrovascular lesions in spontaneously hypertensive rats. In: *The Cerebral Vessel Wall*. Raven: New York, 1976.

8 Nobili F, Rodriguez G, Marenco S, De Carli F, Gambaro M, Castello C *et al.* Regional cerebral blood flow in chronic hypertension. A correlative study. *Stroke* 1993; **24**: 1148–1153.
9 Efimova IY, Efimova NY, Triss SV, Lishmanov YB. Brain perfusion and cognitive function changes in hypertensive patients. *Hypertens Res* 2008; **31**: 673–678.
10 Fujishima M, Ibayashi S, Fujii K, Mori S. Cerebral blood flow and brain function in hypertension. *Hypertens Res* 1995; **18**: 111–117.
11 Jennings JR, Muldoon MF, Ryan C, Price JC, Greer P, Sutton-Tyrrell K *et al.* Reduced cerebral blood flow response and compensation among patients with untreated hypertension. *Neurology* 2005; **64**: 1358–1365.
12 Kety SS, Hafkenschiel JH, Jeffers WA, Leopold IH, Shenkin HA. The blood flow, vascular resistance, and oxygen consumption of the brain in essential hypertension. *J Clin Invest* 1948; **27**: 511–514.
13 Lassen NA. Cerebral blood flow and oxygen consumption in man. *Physiol Rev* 1959; **39**: 183–238.
14 Yamori Y, Horie R. Developmental course of hypertension and regional cerebral blood flow in stroke-prone spontaneously hypertensive rats. *Stroke* 1977; **8**: 456–461.
15 Maeda H, Matsumoto M, Handa N, Hougaku H, Ogawa S, Itoh T *et al.* Reactivity of cerebral blood flow to carbon dioxide in hypertensive patients: evaluation by the transcranial Doppler method. *J Hypertens* 1994; **12**: 191–197.
16 Kim T, Hendrich K, Kim SG. Functional MRI with magnetization transfer effects: determination of BOLD and arterial blood volume changes. *Magn Reson Med* 2008; **60**: 1518–1523.
17 Kim T, Kim SG. Quantification of cerebral arterial blood volume and cerebral blood flow using MRI with modulation of tissue and vessel (MOTIVE) signals. *Magn Reson Medi* 2005; **54**: 333–342.
18 Kim T, Kim SG. Temporal dynamics and spatial specificity of arterial and venous blood volume changes during visual stimulation: implication for BOLD quantification. *J Cereb Blood Flow Metab* 2011; **31**: 1211–1222.
19 Kim T, Hendrich KS, Masamoto K, Kim SG. Arterial versus total blood volume changes during neural activity-induced cerebral blood flow change: implication for BOLD fMRI. *J Cereb Blood Flow Metab* 2007; **27**: 1235–1247.
20 Paxinos G, Watson C (eds) *The Rat Brain in Stereotaxic Coordinates*. Academic Press Incorporated: New York, 2005.
21 Herscovitch P, Raichle ME. What is the correct value for the brain--blood partition coefficient for water? *J Cereb Blood Flow Metab* 1985; **5**: 65–69.
22 Kim T, Kim SG. Quantification of cerebral arterial blood volume using arterial spin labeling with intravoxel incoherent motion-sensitive gradients. *Magn Reson Med* 2006; **55**: 1047–1057.
23 Kim T, Kim SG. *Dynamics of Arterial Labeled Spins Investigated by using 2-coil DASL*. *Proc 10th Annual Meeting*. ISMRM: Hawaii, USA, 2002, p.1061.
24 Kim T, Kim SG. Cortical layer-dependent arterial blood volume changes: improved spatial specificity relative to BOLD fMRI. *Neuroimage* 2010; **49**: 1340–1349.
25 Bendel P, Eilam R. Quantitation of ventricular size in normal and spontaneously hypertensive rats by magnetic resonance imaging. *Brain Res* 1992; **574**: 224–228.
26 Tajima A, Hans FJ, Livingstone D, Wei L, Finnegan W, DeMaro J *et al.* Smaller local brain volumes and cerebral atrophy in spontaneously hypertensive rats. *Hypertension* 1993; **21**: 105–111.
27 Ritter S, Dinh TT. Progressive postnatal dilation of brain ventricles in spontaneously hypertensive rats. *Brain Res* 1986; **370**: 327–332.
28 Sabbatini M, Strocchi P, Vitaioli L, Amenta F. Microanatomical changes of intracerebral arteries in spontaneously hypertensive rats: a model of cerebrovascular disease of the elderly. *Mechan Ageing Dev* 2001; **122**: 1257–1268.
29 Sabbatini M, Catalani A, Consoli C, Marletta N, Tomassoni D, Avola R. The hippocampus in spontaneously hypertensive rats: an animal model of vascular dementia? *Mech Ageing Dev* 2002; **123**: 547–559.
30 Leoni RF, Paiva FF, Henning EC, Nascimento GC, Tannus A, de Araujo DB *et al.* Magnetic resonance imaging quantification of regional cerebral blood flow and cerebrovascular reactivity to carbon dioxide in normotensive and hypertensive rats. *Neuroimage* 2011; **58**: 75–81.
31 Danker JF, Duong TQ. Quantitative regional cerebral blood flow MRI of animal model of attention-deficit/hyperactivity disorder. *Brain Res* 2007; **1150**: 217–224.
32 Chillon J-M, Baumbach G. Autoregulation of cerebral blood flow. In: Welch K, Caplan L, Reis D, Siesjo B, Weir B (eds) *Primer on Cerebrovascular Diseases*. Acadmic Press: San Diego, 1997, pp 51–54.
33 Cohen ER, Ugurbil K, Kim SG. Effect of basal conditions on the magnitude and dynamics of the blood oxygenation level-dependent fMRI response. *J Cereb Blood FlowMetab* 2002; **22**: 1042–1053.
34 Tominaga S, Strandgaard S, Uemura K, Ito K, Kutsuzawa T. Cerebrovascular CO2 reactivity in normotensive and hypertensive man. *Stroke* 1976; **7**: 507–510.
35 Harper SL, Bohlen HG. Microvascular adaptation in the cerebral cortex of adult spontaneously hypertensive rats. *Hypertension* 1984; **6**: 408–419.
36 Saito H, Togashi H, Yoshioka M, Nakamura N, Minami M, Parvez H. Animal models of vascular dementia with emphasis on stroke-prone spontaneously hypertensive rats. *Clin Exp Pharmacol Physiol Suppl* 1995; **22**: S257–S259.
37 Kimura S, Saito H, Minami M, Togashi H, Nakamura N, Nemoto M *et al.* Pathogenesis of vascular dementia in stroke-prone spontaneously hypertensive rats. *Toxicology* 2000; **153**: 167–178.
38 Nabika T, Cui Z, Masuda J. The stroke-prone spontaneously hypertensive rat: how good is it as a model for cerebrovascular diseases? *Cell Mol Neurobiol* 2004; **24**: 639–646.
39 Amenta F, Di Tullio MA, Tomassoni D. Arterial hypertension and brain damage--evidence from animal models (review). *Clin Exp Hypertens* 2003; **25**: 359–380.